RSC Advances

Thermal stablility of p-dimethylaminophenylpentazole

Journal:	*RSC Advances*
Manuscript ID:	RA-ART-08-2014-008454.R1
Article Type:	Paper
Date Submitted by the Author:	23-Oct-2014
Complete List of Authors:	Yang, Yu-Zhang; Beijing Institute of Technology, School of Materials Science and Engineering Pang, Si-Ping; Beijing Institute of Technolodgy, ; Beijing Institute of Technology, School of Materials Science and Engineering Li, Yu-chuan; Beijing Institute of Technology, School of Materials Science & Engineering; Henan Institute of Science and Technology, School of Life Science Zhang, Ru bo; Beijing Institute of Technology, School of Chemistry Sun, Cheng-Hui; Beijing Institute of Technolodgy, School of Material Science & Engineering

Table of contents entry

A thorough thermal stability study of *p*-dimethylaminophenylpentazole was investigated through integration of rapid, stepwise and constant heating model.

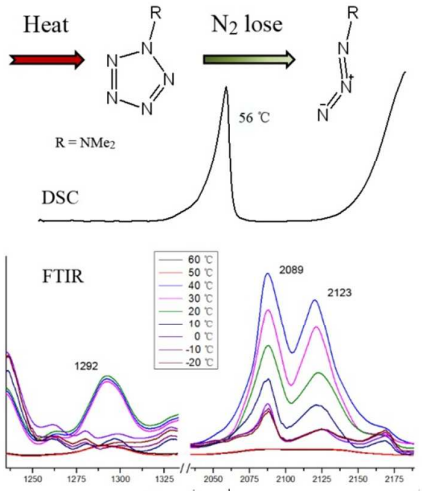

Journal Name

RSCPublishing

paper

Thermal Stability of *p*-Dimethylaminophenylpentazole

Yu-zhang Yang[a], Yu-chuan Li[a], Ru-bo Zhang[b], Cheng-hui Sun[a] and Si-ping Pang[a*]

Cite this: DOI: xxxxx/x0xx00000x

Received 00th January 201x,
Accepted 00th January 201x

DOI: xxxxx/x0xx00000x

www.rsc.org/

The thermal stability of *p*-dimethylaminophenylpentazole (**1**) in the solid phase has been thoroughly investigated. The decomposition process of 1 has been verified by a combination of differential scanning calorimetry (DSC), thin-layer chromatography (TLC), temperature-programmed FTIR, and Raman spectroscopy. FTIR and Raman spectra were also calculated to corroborate the results. It was found that **1** could be handled below 20 °C without any obvious deterioration, but it decomposed sharply at 56 °C. The calculated FTIR and Raman vibrational frequencies were in accord with the experimental values.

Introduction[1]

Pentazole[1-8] is an elusive and attractive compound, which represents the final member of the azole family. As an energy-containing material[9-11] as well as a potential precursor for other polynitrogen compounds,[11-14] pentazole has motivated a great deal of research recently. In particular, the cyclo-N_5 anion is worthy of research as a cycle completely composed of nitrogen.[9,16-18] However, cyclo-N_5 has yet to be unequivocally identified, other than by mass spectrometric detection under high collision voltage and laser ionization by Vij[19] and Östmark,[20] respectively. A claim to the contrary by Butler et al.[21] was subsequently shown to be erroneous,[22] and the cyclo-N_5 anion has not yet been observed in the bulk state. Estimates of the thermal stability of the pentazole anion also vary greatly.[4,12,14,16] Further studies are necessary to characterize this elusive compound.

As key precursors of the pentazole anion, even the decomposition behavior of arylpentazoles remains unexplored. The crystal structure of *p*-dimethylaminophenylpentazole, the most stable known arylpentazole,[27] was reported in 1983.[28] It does not decompose over many hours at 243 K in solution. IR experiments[29] revealed that the nitrogen-loss decomposition process occurs through laser excitation rather than thermodynamic change. Other spectroscopic studies[23,30] also showed its unstable nature, see scheme 1. In previous work, NMR spectra[23] showed a short lifetime of about 30 min at -5 °C, and other experiments[1,4,5,24] gave similar results. However, pertinent experimental investigations and reliable experimental data on the

a School of Materilas Science & Engineering
Beijing Institute of Technology
South Street No. 5, Zhongguancun
Haidian District, 100081 Beijing (China)
E-mail: pangsp@bit.edu.cn
Homepage: http://pnc.bit.edu.cn/
b School of Chemistry, Beijing Institute of Technology
South Street No. 5, Zhongguancun, Haidian District
100081 Beijing (China)

† Electronic Supplementary Information (ESI) available: Synthesis procedure, NMR data, Mass spectra, Single crystal X-ray diffraction and Calculation detail. See DOI: xxxxx/x0xx00000x.

thermal stability are lacking, especially in the solid phase. It is not clear exactly at what temperature **1** would undergo decomposition and over what temperature range it could be treated,[23,25,26] which has obstructed further research on pentazole chemistry. In this context, study of the decomposition process, and the correlation between stability and temperature of **1** is imperative, since it could provide us not only with a helpful measure to understand this metastable substance, but also a necessary and valuable foundation for further research.

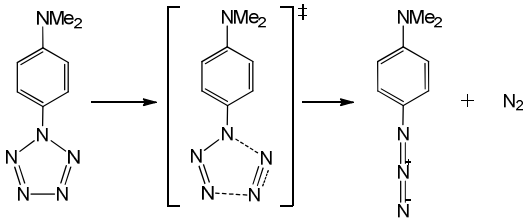

Scheme 1. Decomposition of *p*-dimethylaminophenylpentazole (**1**).

In the present work, the thermal stability of *p*-dimethylaminophenylpentazole (**1**) has been investigated in the solid phase. The thermal decomposition process has been analyzed by differential scanning calorimetry (DSC) and thin-layer chromatography (TLC), as well as by temperature-programmed Fourier-transform IR (FTIR) and Raman spectroscopy.

Experimental

Synthesis and purification

p-Dimethylaminophenylpentazole (**1**) was prepared by a method similar to that used previously.[20] The crude product **1** was first washed with methanol and diethyl ether. Needle-shaped crystals of **1** were obtained by liquid diffusion of diethyl ether and dichloromethane. *p*-Dimethylaminophenylazide (**2**) was obtained by pyrolysis of **1** under exclusion of light (scheme 2).

Single-crystal analysis

Crystals of **1** suitable for X-ray crystallographic analysis were obtained as outlined above. X-ray diffraction intensity data were collected at 293 K on a Bruker Smart Apex2 CCD area-detector diffractometer using graphite-monochromated Mo-Kα radiation (λ = 0.71069 Å). Intensity data were processed using the Bruker SMART routine.

Thermal analysis

Differential scanning calorimetry (DSC) was carried out on a TA Q2000 system. Ramp rates of 5 °C/min from -50 to 200 °C were used with an N_2 purge gas after an initial 30 min isothermal period at 40 °C to remove atmospheric gases and adsorbed moisture. On account of the volatility of **2**, the container had to be well sealed.

TLC experiments

Silica gel plates (5 cm × 7 cm) were used in thin-layer chromatography experiments, and a mobile phase of ethyl acetate/petroleum ether (1:6, v/v) was selected for developing at -35 °C. Equal amounts of **1** were sealed in several numbered centrifuge tubes, each a group of 10 tubes, and each group was incubated at a different temperature. Before development, each tube was maintained at -35 °C after the specific time of incubation in order to avoid further decomposition. The solution for development was prepared with precooled dichloromethane. Each group of samples developed on a single plate was observed under a UV lamp at 254 nm.

FTIR spectra

FTIR experiments were performed with a Perkin-Elmer Spectrum 400 spectrometer attached to a software-controlled INSTEC STC2000 heating stage. The neat solid **1** was ground with cold potassium bromide (KBr) in a volume ratio of 1:100. The mixture was transferred to a die and after cryodesiccation was pressed at around 20 MPa for 30 s to obtain a clear glassy disk about 1 mm thick. The disk was then carefully fixed on the stage. All

appliances had to be precooled. Spectra were collected in the frequency range 400-4000 cm^{-1}. Test temperature points were -20, -10, 0, 10, 20, 30, 40, 50, and 60 °C. Single spectra were measured with a resolution of 2 cm^{-1} and averaged over 16 individual scans. A constant flow of nitrogen was utilized to guarantee from rapid condensation of water from the air at low temperature.

Raman spectra

Raman spectra were recorded on a Jobin-Yvon HR800 triple spectrometer equipped with a cooled charge-coupled device. In this spectrometer, a long focus objective of 20× magnification is used to focus the laser beam on the sample surface and to collect the scattered light. Raman spectra were excited with 532.0 nm radiation from a coherent solid-state laser. The laser power at the focus spot of about 1 mm in diameter was kept at about 4.8 mW to obtain high-quality spectra and to prevent laser-induced damage of the samples. The frequency range 200-2000 cm^{-1} was scanned.

Computational details

Structure optimization and frequency calculation of **1** and **2** were performed with the Gaussian 09W software package, employing the DFT method at the B3LYP/6-31G(d) level. Optimized geometries and frequency distributions were calculated at 0 K.

Results and discussion

The single-crystal structure and stacking mode of **1** are shown in Figure 1, and crystallographic data are summarized in Table S1. Bond lengths and bond angles are similar to those reported previously.[28] Geometry optimization of **1** was performed by the DFT method at the B3LYP/6-31G(d) level as before. The coplanar arrangement of the pentazole and benzene rings was indicated by the theoretical optimized geometries (Figure S9).

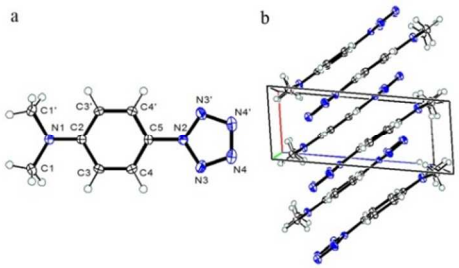

Figure 1. (a) Thermal ellipsoid plot (50% probability) and labeling scheme for **1**. (b) Packing diagram of **1**.

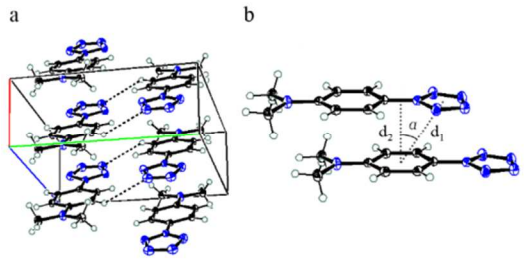

Figure 2. Molecular interactions of **1**. (a) H bond between adjacent rows. (b) π–π interaction of aromatic rings. d_1 = 3.762 Å, d_2 = 3.463 Å, α = 27.551 °.

Actually, at variance with the computational results,[29,32] the two aromatic rings are not in one plane. The two C-N bonds, which are located on the symmetry axis of the C2*v* symmetry molecule, are slightly out of the plane of the benzene ring, making the whole molecule like a bow. The deviation between reality and calculation is not only a result of considering only a single molecule in the calculation whereas molecules are stacked in reality, but also the existence of intermolecular and intramolecular interactions (Figure 2). First, the electron density is increased on the pentazole ring owing to the cooperation of electrophilic pentazole and electrophobic dimethylamino, while it is decreased on the benzene ring. In a given row, the molecular distance is indicative of a π-π interaction between the pentazole and the adjacent benzene in a parallel-displaced disposition.[33] Furthermore, H···N contacts (3.090 Å), corresponding to a heavy-atom C-H···O distance of 3.885 Å with an angle of 142.325°, occur between adjacent rows through C4/C4' and N4/N4'. This structure could be helpful to molecular stability. Besides, potential intramolecular

interaction could weaken the C-N bond under the condition of negative charge transfer caused by the appending of highly electron-donating substituents at the para-position of the phenyl ring.

Differential scanning calorimetry (DSC) periments were carried out to give a direct indication of thermal behavior. In Figure 3, curve ***a*** shows two distinct exothermic steps during testing, while curve ***b*** shows an endothermic peak and an exothermic peak. The endothermic peak at 42 °C proved to be the melting point of compound **2** by a melting point test. Therefore, the broad peak at about 157 °C is related to decomposition of compound **2**. This was verified by mass spectrometry (Figure S4 and S5). It can be concluded that the first exothermic step at about 56 °C in curve ***a*** relates to the decomposition of pentazole. The exothermic reaction takes place at 20 °C and reaches a maximum at 56 °C, indicating that the decomposition is an incrementally increasing exothermic process upon heating. The decompositions of both **1** and **2** are exothermic in nature owing to the formation of the highly stable N_2 molecule.

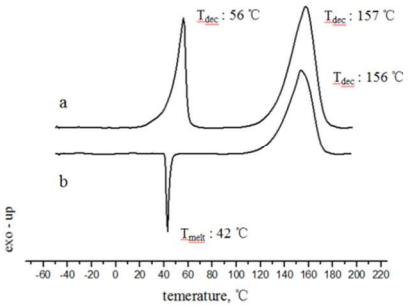

Figure 3. DSC plots of **1** and **2**. Curve ***a*** presents **1**, and ***b*** presents **2**.

As the DSC curves show, exothermic decomposition of pentazole begins at about 20 °C and is enhanced by increasing temperature. It can be deduced that compound **1** may feasibly exist at room temperature for a short time, but for how long it could survive under different circumstances still needs to be explored.

To better understand the thermal stability of **1** at different temperatures, thin-layer chromatography (TLC) experiments were carried out. TLC is generally used for substance separation and reaction tracking. Here, we developed it for monitoring the decomposition process of **1** by taking advantage of the coloration imparted by the organic product on silica gel.

Figure 4 illustrates the development of the treated samples. The Rf value of **1** is smaller than that of **2** because the polarity of the arylpentazole is greater than that of the corresponding azide. The degree of decomposition of **1** could be estimated from the intensity of the less mobile spots. The respective plates displayed the results at different temperatures.

At a fixed temperature, on plate A, the less mobile spots gradually diminished in intensity as a result of reduction in the content of **1**, implying the transformation of **1** to **2**. However, the more mobile spots appeared almost unchanged in intensity due to the outstanding color rendering of **2** under UV light. Although each plate demonstrated the same variation tendency, the decomposition rates of **1** were quite different. At 0 °C, **1** could exist for about 3 days. At 20 °C, **1** decomposed completely in about 270 min. At 50 °C, however, the spots of **1** disappeared within 5 min. It could be concluded that the higher the temperature, the shorter the time needed for the spots of **1** to completely disappear. The thermal stability of **1** was clearly lower at 20 °C than at 0 °C, but not so severely as to preclude its handling at this temperature. Interestingly, all spots became pink when exposed to sunlight owing to the photolysis of **2**.[31] Thus, it is recommended that all manipulations should be performed under exclusion of light. Mass spectra indicated formation of the same product **2** by both pyrolysis and photolysis (Figure S6).

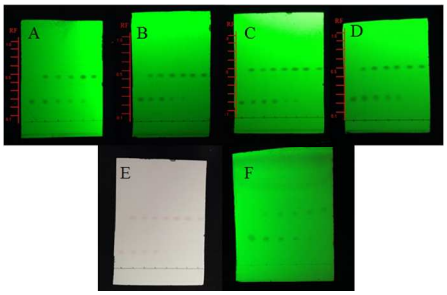

Figure 4. TLC results of **1** and **2**. Plate A, B, C and D show developments at 20 °C, 30 °C, 40 °C, 50 °C, respectively. Time interval of pointing samples on A, B, C and D are 50, 10, 2.5 and 1.2 min, respectively. Bottom spots represent **1**, while uppers represent **2**. Plate E shows photolysis of **2**. Plant F shows development at 0 °C which time interval is 15h.

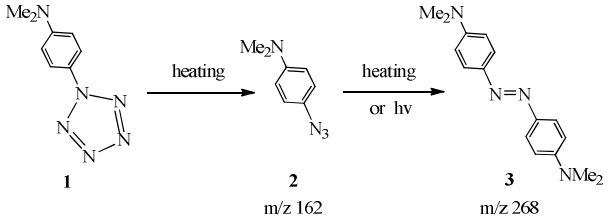

Scheme 2. Pyrolysis of **1** and photolysis of **2**.

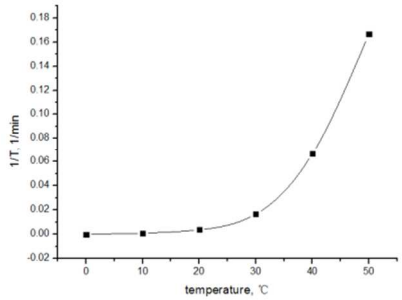

Figure 5. Fitting line of temperatures (X axis) and reciprocal of decomposition times (Y axis).

In Figure 5, a reasonable line accounting for the decomposition tendency is given by fitting the temperatures and reciprocal of decomposition time. The reciprocal is proportional to the decomposition rate. The slope of the line begins to change at about 20 °C, and increases with increasing temperature. The appearance of the line is similar to the DSC curve of **1** in this temperature range. The two ascending phenomena demonstrate the decomposition tendency of compound **1**. It could be concluded that **1** is stable below 0 °C, and this temperature range is considered to be ideal for its treatment and preservation. In the range 0-20 °C, despite a slight effect on decomposition, operating and testing of **1** could be achieved in a reasonable time frame. However, it is difficult to handle **1** at 50 °C on account of its ease of decomposition.

Infrared spectroscopy has been widely used in tracing reaction process,[34] probing intermediates[29,35] and unstable compounds.[36] Raman spectroscopy also has been applied for testing labile materials extensively.[30,37] Both of the two are considered to be suitable for our work. Picosecond-level IR spectroscopic studies[29] and Raman[30] of **1** were performed by Portius and Haas, respectively. Both studies were aimed at displaying the spectra before and after decomposition, and demonstrated a significant difference due to the generation of **2** by the decomposition of **1**. Moreover, they provided a more accurate decomposition temperature of **1**. To further confirm the thermal stability of **1**, we investigated its decomposition process by means of temperature-programmed FTIR and Raman spectroscopies. Frequency calculations of **1** and **2** were also carried out for comparison with the experimental results.

The FTIR spectra are shown in Figure 6. Temperature was increased at a rate of 20 °C/min between each adjacent test point, and there was an unavoidable deviation of 1-2 °C owing to the time required for each scan. Some distinct changes were evident from the curves. The fact that the curves were undefined in the temperature range from -20 to 0 °C is consistent with no decomposition of **1**. However, at higher temperatures, the peaks at ν=2089, 2123, and 1292 cm^{-1} increased sharply. These growing peaks could be assigned to N=N=N asymmetric and symmetric stretching vibrations of azide. Therefore, compound **2** was confirmed to be generated with increasing temperature, and the related peaks are only shown in

spectra above 0 °C. This phenomenon is similar to that which happened in CH_2Cl_2 after fs excitation.[29] However, vibrations attributable to pentazole were calculated to be very weak and indeed were not observed experimentally. Hence, the decomposition of **1** could be monitored by following the growth of the azide peaks. After heating, the sample was cooled to 298 K, but no signal changes were observed. It appears that the transformation from **1** to **2** is irreversible, consistent with the mechanism of the decomposition of arylpentazole.[25] In light of the exothermic peak at 56 °C in the DSC plot of **1**, spectra were recorded at 50 and 60 °C. However, extremely weak spectra were obtained due to volatilization of **2**.

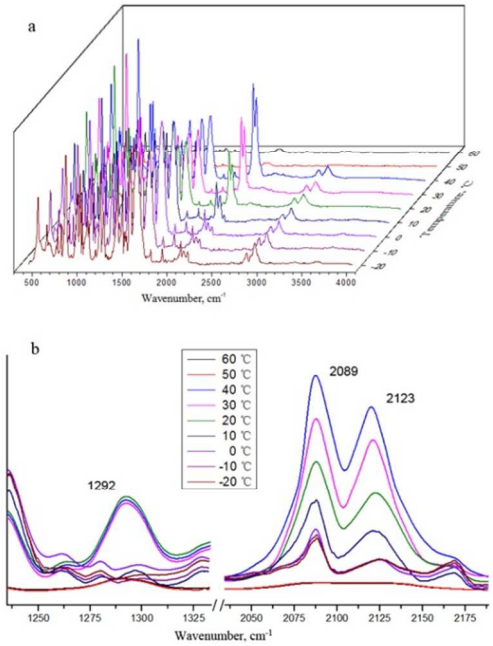

Figure 6. Temperature-programed FTIR spectra of **1**. (a) 3D plot of FTIR spectra recorded at different temperatures. (b) FTIR spectra of **1** recorded in $\nu(N_3)$ stretch region during heating.

Temperature-programmed Raman spectra recorded in the same temperature range are shown in Figure 7. A similar phenomenon to that detected by FTIR spectra was evident. However, the whole curve appeared to be flat during heating. This could be attributed to a lattice energy change. A melting phenomenon was observed at 20 °C during tests. This is a disadvantage of laser focusing in reflected light experiments, unlike for FTIR, which utilizes samples in KBr and transmitted light.

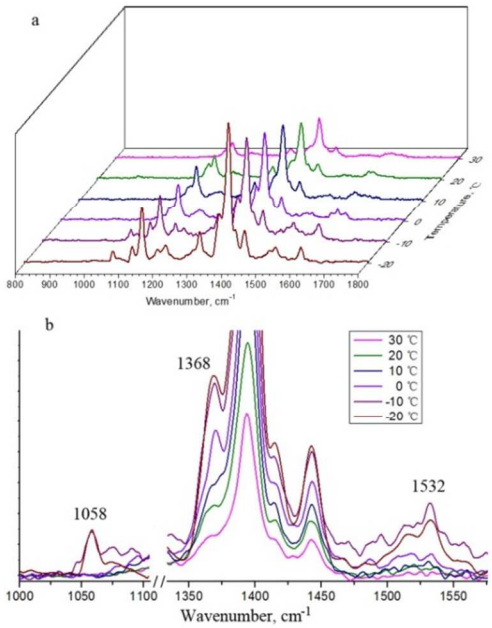

Figure 7. Temperature-programed Raman spectra of **1**. (a) 3D plot of Raman spectra recorded at different temperatures. (b) Raman spectra of **1** recorded in $\nu(N_5)$ stretch region during heating.

In computational results (Figure S10 and S11), all harmonic frequencies relating to the pentazole ring were very small, in accordance with the experimental values. Therefore, the characteristic frequency of azide can be regarded as a judgement basis of the decomposition.

Changes in the FTIR and Raman spectra indicated that **1** underwent a thermal transformation during programmed heating. All changes took place above 0 °C, and they were irreversible. Based on the mechanism of decomposition of arylpentazole in Scheme 2, it is a reasonable explanation that the spectral changes were caused by the decomposition of **1**. Intensive growth of the peaks due to **2** provided clear evidence for the decomposition process. FTIR spectra were compared to the DSC plots. The temperatures at which the curves began to change were slightly different. The temperature point of growth of peak intensity of **2** in FTIR spectra was earlier than that of the onset of exothermic decomposition of **1** by DSC. The explanation for this

discrepancy might be the different operational steps of the two techniques. FTIR spectroscopy is a test process that needs a holding time for scanning, it provides **1** enough time to decompose, whereas DSC is a continuous and rapid procedure which delay temperature response of samples. In addition, spectroscopy is sensitive to functional groups, and therefore the DSC signal is initially delayed relative to the spectroscopic signal. Logically, the thermal stability of **1** is dependent on temperature and time. The longer the exposure at high temperature, the faster the decomposition happens.

Conclusions

The experiments described above have provided clear insight into the thermal stability of **1** in the solid state. Temperatures below 0 °C are safe for its treatment and preservation. At 20 °C, it can still be handled in expeditious operations, but at 50 °C its instability becomes unacceptable. This work thus provides reliable guidelines for selecting the conditions in further research. The thermal analysis of **1** has been integrated with rapid heating (DSC), stepwise heating (FTIR and Raman), and constant temperature (TLC) models. The consistent results obtained have demonstrated the feasibility of this methodology for studying such a metastable substance.

Acknowledgements

The authors gratefully acknowledge the support of the Foundation of NSAF (No.11176004).

References

1 R. Huisgen and I. Ugi, *Chem. Ber.,* 1957, **90**, 2914.

2 R. Huisgen and I. Ugi, *Chem. Ber.,* 1958, **91**, 531.

3 I. Ugi, *Angew. Chem.* 1961, **73**, 172.

4 V. Benin, P. Kaszynski, and J. G. Radziszewski, *J. Org. Chem.,* 2002, **67**, 1354.

5 F. Biesemeier, K. Harms, and U. Müller, *Z. Anorg. Allg. Chem.,* 2004, **630**, 787.

6 R. N. Butler, J. M. Hanniffy, J. C. Stephens, and L. A. Burke, *J. Org. Chem.,* 2008, **73**, 1354.

7 M. Witanowski, L. Stefaniak, H. Januszewski, and K. Bahadur, *J. Cryst. Mol. Struct.,* 1975, **5**, 137.

8 P. Carlqvist, H. Östmark, and T. Brinck, *J. Phys. Chem.,* 2004, **108**, 7463.

9 I. S. O. Pimienta, S. Elzey, J. A. Boatz, and M. S. Gordon, *J. Phys. Chem. A*, 2007, **111**, 691.

10 S. A. Perera, A. Gregušová, and R. J. Bartlett, *J. Phys. Chem. A*, 2009, **113**, 3197.

11 Y. Xu, F. J. Zhao, Y. Zhang, Y. L. Gu, T. X. Liu, and J. Cui, *Int. J. Quantum Chem.,* 2010, **110**, 1135.

12 S. Fau, K. J. Wilson, and R. J. Bartlett, *J. Phys. Chem. A*, 2002, **106**, 4639.

13 M. N. Glukhovtsev, P. von R. Schleyer, and C. Maerker, *J. Phys. Chem*., 1993, **97**, 8200.

14 K. O. Christe, *Prop., Explos., Pyrotech.,* 2007, **32**, 194.

15 M. N. Glukhovtsev, H. J. Jiao, and P. von R. Schleyer, *Inorg. Chem.,* 1996, **35**, 7124.

16 K. F. Ferrist and R. J. Bartlett, *J. Am. Chem. Soc*., 1992, **114**, 8302.

17 L. A. Burke, R. N. Butler, and J. C. Stephens, *J. Chem. Soc., Perkin Trans.,* 2001, **2**, 1679.

18 G. Frison, G. Jacob, and G. Ohanessian, *New J. Chem.,* 2013, **37**, 611.

19 A. Vij, J. G. Pavlovich, W. W. Wilson, V. Vij, and K. O. Christe, *Angew. Chem*., 2002, **114**, 3177.

20 H. Östmark, S. Wallin, T. Brinck, P. Carlqvist, R. Claridge, E. Hedlund, and L. Yudina, *Chem. Phys. Lett.,* 2003, **379**, 539.

21 R. N. Butler, J. C. Stephens, and L. A. Burke, *Chem. Commun.,* 2003, 1016.

22 T. Schroer, R. Haiges, S. Schneider, and K. O. Christe, *Chem. Commun.,* 2005, 1607.

23 R. N. Butler, S. Collier, and A. F. M. Fleming, *J. Chem. Soc., Perkin Trans.,* 1996, **2**, 801.

24 J. L. Zhang, S. P. Pang, Y. C. Li, Y. Z. Yu, and H. J. Zhang, *Chinese Journal of Energetic Materials,* 2006, **14**, 355.

25 R. N. Butler, A. Fox, S. Collier, and L. A. Burke, *J. Chem. Soc., Perkin Trans.,* 1998, **2**, 2243.

26 R. N. Butler, J. C. Stephens, and J. M. Hanniffy, *Tetrahedron. Lett.,* 2004, **45**, 1977.

27 I. Ugi, *Advances in Heterocyclic Chemistry* (Ed.: A. R. Katritzky), *Academic Press, New York*, 1964, 373.

28 J. D. Wallis and J. D. Dunitz, *J. Chem. Soc., Chem. Commun.,* 1983, 910.

29 P. Portius, M. Davis, R. Campbell, F. Hartl, Q. Zeng, A. J. H. M. Meijer, and M. Towrie, *J. Phys. Chem. A,* 2013, **117**, 12759.

30 U. Geiger, A. Elyashiv, R. Fraenkel, S. Zilberg, and Y. Haas, *Chem. Phys. Lett.,* 2013, **556**, 127.

31 Y. Z. Li, J. P. Kirby, M. W. George, M. Poliakoff, and G. B. Schuster, *J. Am. Chem. Soc.,* 1988, **110**, 8092.

32 L. Belau, Y. Haas, S. Zilberg, *J. Phys. Chem.,* 2004, **108**, 11715.

33 (a) C. Janiak, *J. Chem. Soc., Dalton Trans.*, 2000, 3885. (b) S. A. Arnstein and C. D. Sherrill, *Phys.Chem.Chem.Phys.*, 2008, **10**, 2646. (c) J. I. Seo, I. Kim, Y. S. Lee, *Chem. Phys. Lett.,* 2009, **474**, 101.

34 (a) A. Sharma, I. Reva, R. Fausto, S. Hesse, Z. F. Xue, M. A. Suhm, S. K. Nayak, R. Sathishkumar, R. Pal, and T. N. Guru Row, *J. Am. Soc.*, 2011, **133**, 20194. (b) N. Mozhzhukhina, L. P. Méndez De Leo, and E. J. Calvo, *J. Phys. Chem*., 2013, **117**, 18375.

35 J. Jašík, D. Gerlich, and J. Roithová, *J. Am. Soc.*, 2014, **136**, 2960.

36 (a) A. Vij, W. W. Wilson, V. Vij, F. S. Tham, J. A. Sheehy, and K. O. Christe, *J. Am. Soc.*, 2001, **123**, 6308. (b) X. Q. Zeng, H. Beckers, and H. Willer, *Angew. Chem. Int. Ed.* 2013, **52**, 1.

37 (a) K. O. Christe, W. W. Wilson, J. A. Sheehy, and J. A. Boatz, *Angew. Chem. Int. Ed.* 1999, **38**, 13. (b) X. Q. Zeng, H. Beckers, H. Willner, and J. F. Stanton, *Eur. J. Inorg. Chem.* 2012, **21**, 3403.